

Partially Coherent EGC Reception of Uncoded and LDPC-Coded Signals over Generalized Fading Channels

Goran T. Djordjevic · Ivan B. Djordjevic ·
George K. Karagiannidis

Published online: 21 April 2011
© Springer Science+Business Media, LLC. 2011

Abstract This paper studies the bit-error rate (BER) performance of partially coherent equal-gain combining reception of uncoded and low-density parity-check (LDPC)-coded binary and quaternary phase-shift keying signals over generalized $\alpha - \mu$ fading channels. For the uncoded signal detection case the obtained numerical and simulation results illustrate the BER performance degradation due to the imperfect reference signal recovery, receiver unbalancing and fading. It is demonstrated that imperfect cophasing causes an irreducible BER performance. Furthermore, we design large girth quasi-cyclic LDPC code with high code rate, suitable for use in communications over generalized fading channels. The proposed LDPC code does not exhibit the error floor phenomena, in the region of interest, even in the presence of imperfect cophasing and receiver unbalances, and outperforms standard convolutional code of lower code rate in the observed impairments. The effects of number of iterations in decoding algorithm and codeword length on BER performance are also investigated.

A part of this paper was presented at IEEE WCNC 2009.

G. T. Djordjevic (✉)
Department of Telecommunications, Faculty of Electronic Engineering, University of Nis,
Aleksandra Medvedeva 14, 18000 Nis, Serbia
e-mail: goran@elfak.ni.ac.rs

I. B. Djordjevic
Department of Electrical and Computer Engineering, University of Arizona,
1230 E. Speedway Blvd., Tucson, AZ 85721, USA
e-mail: ivan@ece.arizona.edu

G. K. Karagiannidis
Department of Electrical and Computer Engineering, Aristotle University of Thessaloniki,
Thessaloniki 54 124, Greece
e-mail: geokarag@auth.gr

Keywords Bit-error rate · Equal-gain combining · Low-density parity-check (LDPC) codes · Phase error · Phase-shift keying

1 Introduction

Space diversity reception techniques are useful tools for mitigating the deleterious effects of fading in wireless communication systems. The equal-gain combining (EGC) receiver achieves a comparable bit-error rate (BER) performance compared with the optimum maximum ratio combining (MRC) receiver, but on the other hand it has lower implementation complexity than that of MRC because it does not require estimation of the fading envelopes. According to the EGC technique, the received signals at all branches are cophased, equally weighted and summed to give the resultant output signal [1].

Previous papers concerning EGC diversity [2–5] (and references therein) assumed the received signal phase estimation to be perfect. Only three papers, [6–8], considered the influence of imperfect estimation of the received signal phase on the system performance. The authors in [6] discussed the phase error influence on the BER values in detecting binary and quaternary phase-shift keying (BPSK and QPSK) signals. The analysis was done under the assumption of identical and statistically independent Rayleigh fading. In [7] the authors derived closed-form expressions for the outage probability and average BER in detecting BPSK and QPSK signals transmitted over correlated Nakagami- m fading channels. The EGC technique with dual branches was also observed in that paper. In [8], a new method was developed to analyze the average BER and signal-to-noise (SNR) reliability performance of partially coherent BPSK and QPSK systems under multibranch EGC diversity reception over Rayleigh, Rician and Nakagami- m fading.

In this paper, we study the performance of unbalanced EGC receivers with imperfect cophasing, operating over non-identical generalized $\alpha - \mu$ (or generalized Gamma) fading channels [9,10] with arbitrary values of parameters. The difference between the incoming and the estimated signal phase is a stochastic process that is assumed to follow the Tikhonov distribution, as in [6–8,11]. Notice that the Nakagami- m , exponential, Weibull, one-sided Gaussian and Rayleigh distribution that are used for modeling multipath fading channels, as well as Gamma and Lognormal (as a limiting case) distributions that are used for modeling shadow fading are special instances of the generalized $\alpha - \mu$ distribution [9,10]. Despite the fact that the $\alpha - \mu$ distribution includes several widely used fading distributions as special cases, only two papers [4,5] considered the performance of EGC receiver in $\alpha - \mu$ fading channel, and analysis in both papers was done under assumption of perfect cophasing. Unlike previously mentioned papers [2–8], where the uncoded signal detection was observed, in this paper we determine the average BER for both uncoded and low-density parity-check (LDPC)-coded BPSK and QPSK signals. To facilitate the implementation at high-speeds the LDPC codes are designed in quasi-cyclic fashion. To avoid the error floor phenomena for transmission over the generalized fading channels in the presence of imperfect phase recovery and receiver unbalances, the LDPC codes of large girth are employed.

The rest of the paper is organized as follows. Section 2 describes the system model, the LDPC code design, and the description of evaluation of symbol and bit reliabilities. The numerical results, followed by discussions, are presented in Sect. 3. Section 4 contains the summary of the main results and provides some concluding remarks.

2 System and Channel Model

2.1 Channel Model

According to the generalized fading channel model, the signal envelope at the i -th receiver branch (Fig. 1) follows $\alpha - \mu$ distribution with probability density function (PDF) given by [9, 10]

$$p_{r_i}(r_i) = \frac{\alpha_i \mu_i^{\mu_i} r_i^{\alpha_i \mu_i - 1}}{\hat{r}_i^{\alpha_i \mu_i} \Gamma(\mu_i)} \exp\left(\mu_i \frac{r_i^{\alpha_i}}{\hat{r}_i^{\alpha_i}}\right), \tag{1}$$

where $\alpha_i > 0$ is the parameter of nonlinearity, $\Gamma(\cdot)$ is the Gamma function [12, eq.(8.310⁷)], and $\mu_i > 0$ is the inverse of the normalized variance of $r_i^{\alpha_i}$

$$\mu_i = \frac{E^2\{r_i^{\alpha_i}\}}{\text{Var}\{r_i^{\alpha_i}\}}, \tag{2}$$

where $E\{\cdot\}$ and $\text{Var}\{\cdot\}$ are the expectation and variance operator, respectively, and \hat{r}_i is a α_i -root mean value

$$\hat{r}_i = \sqrt[\alpha_i]{E\{r_i^{\alpha_i}\}}. \tag{3}$$

2.2 Receiver Model

The signal at the i -th receiver antenna (see Fig. 1) can be written as

$$s_i(t) = r_i(t) e^{j\gamma_i(t)} A e^{j(\omega_0 t + \phi_n)} + n_i(t), \quad i = 1, 2, \dots, L, \tag{4}$$

where $r_i(t)$ is the fading envelope, $\gamma_i(t)$ is the random phase shift occurred during signal transmission over a fading channel. The number of the receiver branches is denoted by L . Each antenna experiences frequency nonselective and slow fading, which is independent from symbol to symbol and there is no correlation between fading on different antennas. The amplitude of useful signal is denoted with A and it can be assumed without loss of generality that it is equal to one. With ϕ_n we denote the signal phase in which information about the symbol is imposed. In the case of the BPSK signal ϕ_n has one of the following values: $\{0, \pi\}$, and in the case of the QPSK signal ϕ_n has one of the following values: $\{\pi/4, 3\pi/4, 5\pi/4, 7\pi/4\}$. The zero mean Gaussian noise with variance σ_i^2 at the i -th receiver branch is denoted with $n_i(t)$. The standard deviation of this Gaussian noise is given by

$$\sigma_i = \sqrt{\frac{E\{r_i^2\}}{2R \log_2(M) 10^{\gamma_{b1}/10} \exp(-\delta(i-1))}}, \tag{5}$$

where R is the code rate (for uncoded signal $R = 1$), M is the number of phase levels, γ_{b1} is the average SNR per information bit for the first receiver branch and is given in decibels, and δ is the receiver unbalance parameter. The receiver operates with the exponentially decaying power delay profile.

After signal cophasing at all branches, the resulting signal after combining is

$$z(t) = \sum_{i=1}^L \left[A r_i(t) e^{j\phi_n} e^{j\varphi_i(t)} + n_i(t) \right], \tag{6}$$

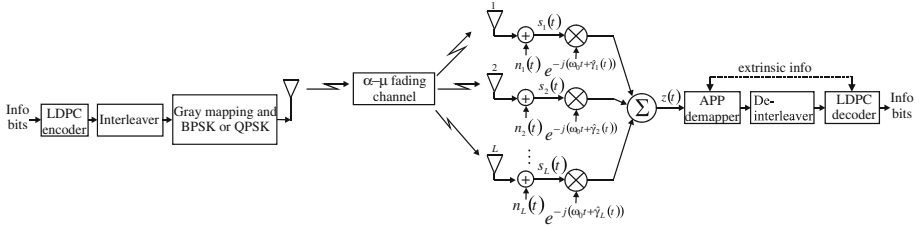


Fig. 1 System model

where L is the number of the receiver branches. The difference between the receiver signal phase $\gamma_i(t)$ at the i -th receiver branch and the estimated phase $\hat{\gamma}_i(t)$ at that receiver branch is denoted with $\varphi_i(t) = \gamma_i(t) - \hat{\gamma}_i(t)$. If the phase estimation is done from unmodulated carrier by using phase-locked loop (PLL) and if only the Gaussian noise is present in the PLL circuit, then the PDF of this phase error is [6–8, 10]

$$p_{\varphi_i}(\varphi_i) = \frac{1}{2\pi} \frac{\exp(\zeta_i \cos(\varphi_i))}{I_0(\zeta_i)}, \quad -\pi < \varphi_i \leq \pi, \tag{7}$$

where $I_0(x)$ is the modified Bessel function of the first kind and zero order for the argument x [12, eq. (8.406)], ζ_i is the SNR in the PLL circuit at the i -th receiver branch, which is related to the phase error variance $\sigma_{\varphi_i}^2$ [6–8, 10] by

$$\zeta_i = \frac{1}{\sigma_{\varphi_i}^2}. \tag{8}$$

The BERs of uncoded BPSK and QPSK signal detection, assuming EGC receiver, are, respectively given by

$$BER = 0.5 \int_{\mathbf{r}} \int_{\boldsymbol{\varphi}} \operatorname{erfc} \left(\frac{\sum_{i=1}^L r_i \cos \varphi_i}{\sqrt{2}\sigma} \right) p_{\boldsymbol{\varphi}}(\boldsymbol{\varphi}) p_{\mathbf{r}}(\mathbf{r}) d\boldsymbol{\varphi} d\mathbf{r} \tag{9}$$

and

$$BER = 0.25 \int_{\mathbf{r}} \int_{\boldsymbol{\varphi}} \left\{ \operatorname{erfc} \left(\frac{\sum_{i=1}^L r_i \cos(\pi/4 - \varphi_i)}{\sqrt{2}\sigma} \right) + \operatorname{erfc} \left(\frac{\sum_{i=1}^L r_i \cos(\pi/4 + \varphi_i)}{\sqrt{2}\sigma} \right) \right\} p_{\boldsymbol{\varphi}}(\boldsymbol{\varphi}) p_{\mathbf{r}}(\mathbf{r}) d\boldsymbol{\varphi} d\mathbf{r}, \tag{10}$$

where

$$\sigma = \sqrt{\sigma_1^2 + \sigma_2^2 + \dots + \sigma_L^2}, \tag{11}$$

$\operatorname{erfc}(\cdot)$ is the complementary error function [12, eq. (7.1.2.)], $p_{\boldsymbol{\varphi}}(\boldsymbol{\varphi})$ is the joint probability density function of the vector $\boldsymbol{\varphi} = (\varphi_1, \varphi_2, \dots, \varphi_L)$, which is, considering that $\varphi_i, i = 1, 2, \dots, L$, are independent, given by

$$p_{\varphi}(\boldsymbol{\varphi}) = \prod_{i=1}^L p_{\varphi_i}(\varphi_i), \tag{12}$$

and $p_{\mathbf{r}}(\mathbf{r})$ is the joint probability density function of the vector $\mathbf{r} = (r_1, r_2, \dots, r_L)$, which is, considering that also $r_i, i = 1, 2, \dots, L$, are independent, given by

$$p_{\mathbf{r}}(\mathbf{r}) = \prod_{i=1}^L p_{r_i}(r_i). \tag{13}$$

2.3 Encoding and Decoding Algorithm

The LDPC codes under study in this paper belong to the class of quasi-cyclic (QC) LDPC codes [13, 14]. The QC codes, lead to encoder that can be implemented based on shift-registers and modulo-2 adders, while complexity of decoder is low compared to random LDPC codes. The parity-check matrix of LDPC codes considered here can be written in the following form

$$H = \begin{bmatrix} I & I & I & \dots & I \\ I & P^{S[1]} & P^{S[2]} & \dots & P^{S[c-1]} \\ I & P^{2S[1]} & P^{2S[2]} & \dots & P^{2S[c-1]} \\ \dots & \dots & \dots & \dots & \dots \\ I & P^{(v-1)S[1]} & P^{(v-1)S[2]} & \dots & P^{(v-1)S[c-1]} \end{bmatrix}, \tag{14}$$

where I is $p \times p$ (p is a prime number) identity matrix, P is $p \times p$ permutation matrix ($p_{i,i+1} = p_{p,1} = 1, i = 1, 2, \dots, p - 1$; other elements of P are zeros), while v and c represent the number of rows and columns in (14), respectively. The set of integers S are to be carefully chosen from the set $\{0, 1, \dots, p - 1\}$ so that the cycles of short length, in corresponding Tanner graph representation of (14) are avoided. The minimum distance for LDPC code is given by the Tanner bound [15]

$$d \geq \begin{cases} 1 + \frac{v}{v-2} \left((v-1)^{\lfloor (g-2)/4 \rfloor} - 1 \right), & g/2 = 2m + 1 \\ 1 + \frac{v}{v-2} \left((v-1)^{\lfloor (g-2)/4 \rfloor} - 1 \right) + (v-1)^{\lfloor (g-2)/4 \rfloor}, & g/2 = 2m \end{cases} \tag{15}$$

where g and v are, respectively the girth of the LDPC code and the column weight of the parity check matrix. The operator $\lfloor \cdot \rfloor$ indicates the largest integer that is smaller or equal to the enclosed number. Equation (15) shows that the linear increase in the girth results in exponentially increase in the minimum distance. Notice that this bound is tight only for short codes (in the order of hundreds), nevertheless it provides a guideline how to design the LDPC codes of large minimum distance. Moreover, the use of large girth LDPC de-correlates the extrinsic information in decoding process.

Example 1 By selecting $p = 673$ and $S = \{0, 2, 5, 13, 20, 37, 58, 91, 135, 160, 220, 525\}$ an LDPC code of rate 0.75, girth $g = 10$, column weight 3 and length $N = 8076$ is obtained.

Example 2 By selecting $p = 360$ and using different indices for the first three block-rows as follows $S_1 = \{5, 275, 310, 13, 19, 284, 3, 2, 151, 176, 46, 218\}$, $S_2 = \{344, 5, 275, 310, 13, 19, 284, 3, 2, 151, 176, 46\}$ and $S_3 = \{151, 334, 275, 13, 284, 2, 176, 218, 5, 310, 19, 3\}$, an LDPC code LDPC (4320, 3242) of rate $R = 0.75$, column weight 3, and girth 8 is obtained.

Example 3 By selecting $p = 593$ and $S = \{0, 2, 7, 3, 30, 38, 65, 97, 138, 158, 239, 436\}$, an LDPC code LDPC (7166, 5339) of rate $R = 0.75$, column weight 3, and girth 8 is obtained.

The decoding algorithm, as mentioned above, is based on sum-product with correction term algorithm [16]. The complexity of this algorithm is low and suitable for field-programmable gate array (FPGA) or very-large-scale integration (VLSI) implementation.

2.4 Symbol and Bit Log-Likelihood Ratios Calculation

The samples of in-phase and quadrature channels are forwarded to the a posteriori probability (APP) demapper, which determines the symbol log-likelihood ratios (LLRs) $\lambda(s)$ by

$$\lambda(s) = -\frac{\{z_I - s_R\}^2}{2\sigma^2} - \frac{\{z_Q - s_Q\}^2}{2\sigma^2}; \quad s = 1, 2, \dots, 2^{n_b} \tag{16}$$

where z_I and z_Q denote the sample of in-phase and quadrature channel outputs (see Eq. (6)), $s = (s_R, s_Q)$ is the constellation point in MPSK constellation diagram, σ^2 denotes the variance of the Gaussian noise process. The number of bits per symbol is denoted by n_b . Let us denote by b_j , the j -th bit in an observed symbol s binary representation $\mathbf{b} = (b_1, b_2, \dots, b_{n_b})$. The bit LLRs required for LDPC decoding are calculated from symbol LLRs by

$$L(b_j) = \log \frac{\sum_{s:b_j=0} \exp(\lambda(s))}{\sum_{s:b_j=1} \exp(\lambda(s))}. \tag{17}$$

Therefore, the j – th bit reliability is calculated as the logarithm of the ratio of a probability that $b_j = 0$ and probability that $b_j = 1$. In the nominator, the summation is done over all symbols s having 0 at the position j , while in the denominator over all symbols s having 1 at the position j . The extrinsic LLRs are iterated backward and forward until convergence or pre-determined number of iterations has been reached, as illustrated in Fig. 1 by dashed arrows.

3 Numerical Results

Without loss of generality, the assumption is that in all receiver branches the phase noise standard deviation is the same: $\sigma_{\varphi_1} = \sigma_{\varphi_2} = \dots = \sigma_{\varphi_L} = \sigma_\varphi$, and the fading parameters are also the same: $\alpha_1 = \alpha_2 = \dots = \alpha_L = \alpha$, $\mu_1 = \mu_2 = \dots = \mu_L = \mu$. For uncoded signal detection we present both numerical results obtained by numerical integration and those obtained by Monte Carlo simulations, and as it is evident there is excellent agreement.

The numerical integration in (9) and (10) was performed by using Gaussian quadrature formulae with previously given precision accuracy.

The simulation model can be summarized as follows. Information bits are uniformly generated and fed into LDPC encoder with encoding process briefly described in the preceding section. The LDPC encoder output bits are Gray mapped and give the information bearing phase ϕ_n . The fading envelope $r_i(t)$ is generated by using following approach. The $\alpha - \mu$ variable, r_i , is related to the Nakagami $- m$ variable, r_{N_i} , by [10]: $r_i^{\alpha_i} = r_{N_i}^2$. It follows that $r_i^{\alpha_i} = \Omega_i$, $\mu_i = m_i(\Omega_i$ and m_i are the parameters of Nakagami $- m$ distribution). The samples with $\alpha - \mu$ distribution are generated by using the algorithm for generating the samples with Gamma distribution from [17, 18], and the previous relation between Nakagami $- m$ (since the Nakagami $- m$ variable is squared root of the Gamma variable) and $\alpha - \mu$ fading variable. The phase error $\varphi_i(t)$ with the Tikhonov PDF is generated by the acceptance/rejection method [19, pp. 381-382]. The σ_{φ_i} is needed for generating the phase error ((7) and (8)). The Gaussian noise $n_i(t)$, from (6), with zero mean and standard deviation given by (5),

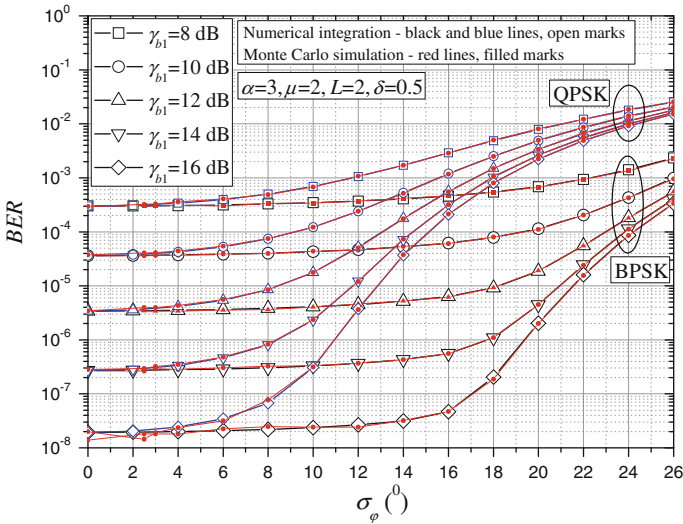


Fig. 2 BER of uncoded BPSK and QPSK as a function of phase error standard deviation

is generated by using the algorithm from [20]. The samples of $z(t)$, given by (6), are fed to the APP demapper, deinterleaver and LDPC decoder that is described in the preceding section. The system model from Fig. 1 incorporates block interleaver and deinterleaver with sufficiently dimension in order to insure the fading samples between two successive symbols are uncorrelated. The numerical results are obtained by applying Monte Carlo simulations. The BER values are estimated on the basis of 3000 information bit errors.

Figure 2 presents the influence of imperfect reference signal phase recovery on BER values in detecting uncoded BPSK and QPSK signals. By setting $\alpha = 3$ and $\mu = 2$, the channel with moderate fading severity is observed. The QPSK modulation format is much more sensitive to the phase error than the BPSK modulation format. In the case of uncoded BPSK, the BER values are constant up to about $\sigma_\varphi = 16^0$, while for uncoded QPSK, BER values start rising always for $\sigma_\varphi = 8^0$.

The influence of EGC receiver unbalance on BER values in detecting uncoded QPSK signals is illustrated in Fig. 3. The unbalance parameter δ considerably influence the BER values in the range of moderate γ_{b1} values. For $\sigma_\varphi = 12.5^0$, in order to achieve $BER = 10^{-5}$ it is necessary to paid γ_{b1} penalty of about 2.8 dB if δ is changed from ideal case to $\delta = 1$. However, in the regime of high values of γ_{b1} , the parameter δ does not influence the BER values that are predominantly influenced by phase noise standard deviation. For $\sigma_\varphi = 12.5^0$ all BER dependences tend to BER floor of about 10^{-6} regardless the amount of EGC receiver unbalance. The value of parameter δ is changed from $\delta = 0$, which relates to perfect balancing case, to $\delta = 2$, corresponding to totally unbalanced branches.

Figure 4 shows the influence of phase error deviation on the average BER values of uncoded and LDPC-coded QPSK signal detection. In the case of uncoded QPSK, the random phase error causes appearance of the BER floor. The values of the phase error standard deviation considerably affect the values of this BER floor. For $\sigma_\varphi = 20^0$, the BER floor value is 10^3 times greater than that for $\sigma_\varphi = 12.5^0$. It is evident that the LDPC code (8076,6059) with high code rate $R = 0.75$ has good performance under considered influences. The simulation results are obtained for 25 iterations in sum-product algorithm. For BER of 10^{-5} ,

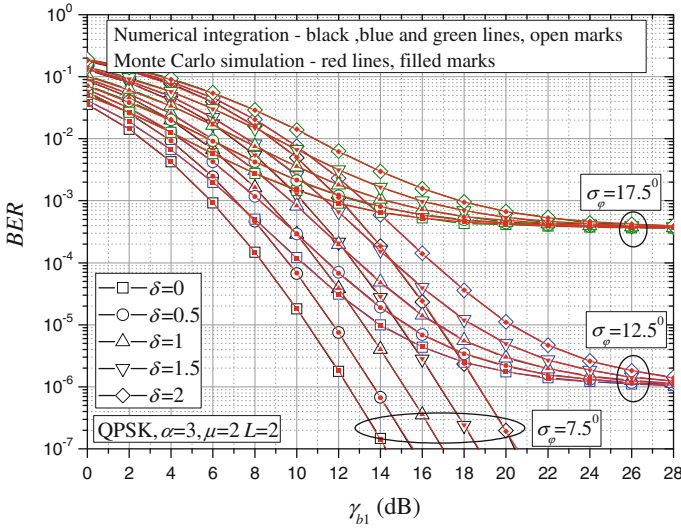


Fig. 3 BER of uncoded QPSK as a function of the average SNR per bit of the first input branch for different values of decaying power delay factor

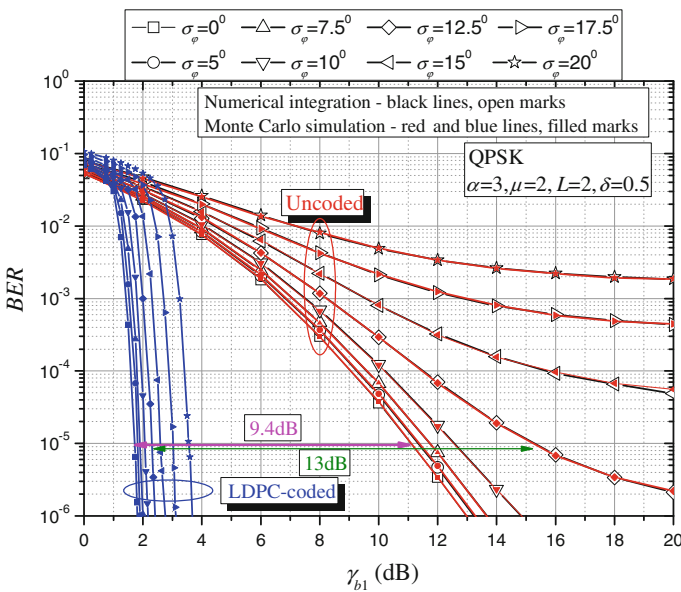


Fig. 4 BER of uncoded and LDPC-coded QPSK as a function of the average SNR per information bit of the first input branch

in the cases of $\sigma_\varphi = 0^0$ and $\sigma_\varphi = 12.5^0$ the corresponding coding gains are 9.4 and 13 dB, respectively. That means that this LDPC code performs very well not only in the generalized fading channel under the influence of unbalancing, but it is also very tolerant to the imperfect cophasing. The higher the value of phase noise standard deviation, the larger the coding gain value is. Notice that this code does not exhibit the BER floor phenomena down to 10^{-6} even

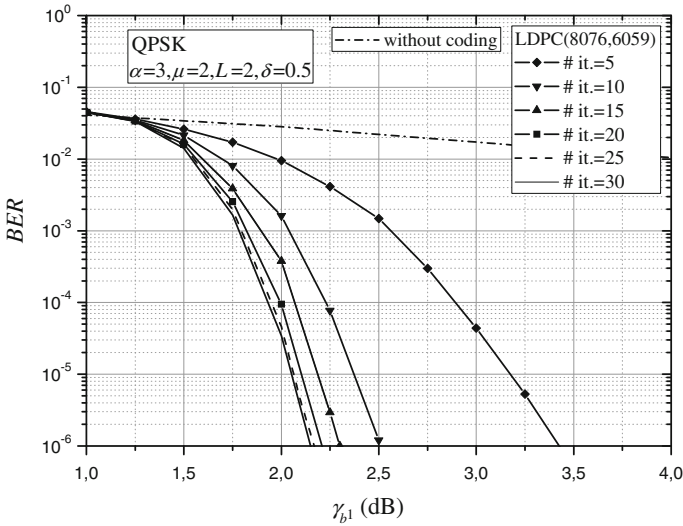


Fig. 5 Effect of number of iterations on LDPC code performance

for $\sigma_\varphi = 20^0$. The reference signal extractor with $\sigma_\varphi \leq 20^0$ can be successfully realized in practice.

Figure 5 illustrates how the LDPC(8076,6059) performance improves as the number of iterations increases. The additional coding gains when number of iterations increases from 5 to 10 and from 15 to 20 are, respectively 0.92 and 0.04 decibels. It is evident that in this channel there is no need to increase the number of iterations greater than 25, because further increasing the number of iterations does not bring any significant coding gain. For given receiver and channel parameters, it is possible to determine the minimum number of iterations in order to achieve the desired BER value. That is important to properly design the decoder with minimum latency for signal processing.

The performance of three LDPC codes of the same code rate and different values of codeword lengths are compared in Fig. 6. The LDPC (8076, 6059) with a codeword length a little bit less than twice that of LDPC (4320, 3248) outperforms it by about 0.3 dB at a BER of 10^{-6} . From a comparison of BER dependences for codes LDPC (7166, 5339) and LDPC (8076, 6059), we conclude that further increase in codeword length leads to little improvement in coding gains. In addition, the codeword length was kept reasonable low to facilitate hardware implementation.

Figure 7 illustrates the influence of diversity order on BER values for both uncoded and LDPC(8076,6059)-coded QPSK signals. The coding gain is greater for smaller number of receiving antennas. Without diversity the BER of 10^{-4} can not be achieved without encoding because the BER floor about 2.5×10^{-4} appears, but with LDPC code application even the lower BER of 10^{-6} is achieved for $\gamma_{b1} = 5$ dB. Similarly, in the case of dual branch diversity, the BER floor slightly greater than 10^{-6} appears for uncoded signals, while with LDPC coding this BER is achieved for $\gamma_{b1} = 1.4$ dB. Table 1 presents the numerical values illustrating the influence of diversity order on BER performance of uncoded and LDPC-coded EGC receiver.

Figure 8 compares the simulation results of the proposed LDPC(8076,6059) code and standard convolutional code CC(2,1,7) with code rate $R = 1/2$, constraint length $K = 7$,

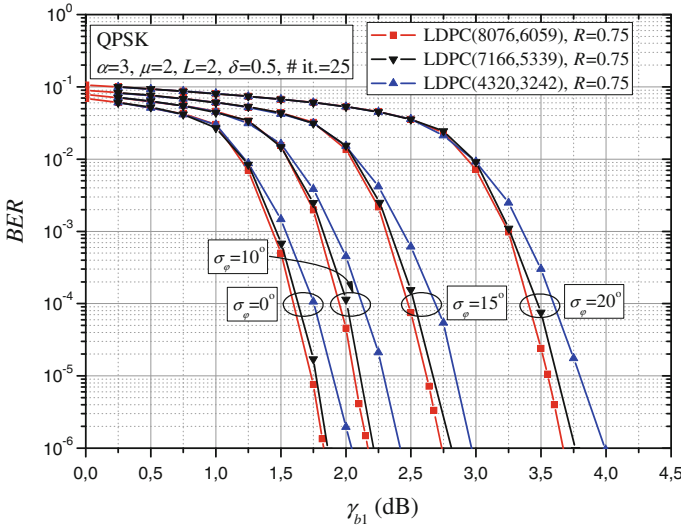


Fig. 6 Effect of LDPC code length on BER performance

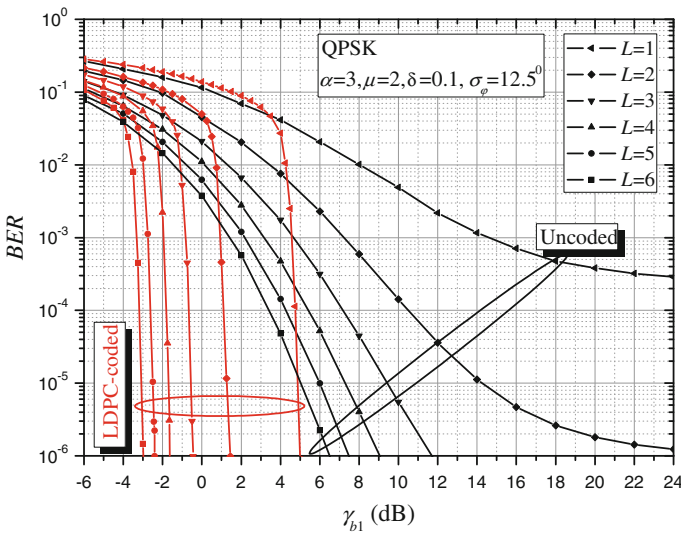


Fig. 7 BER of uncoded and LDPC-coded QPSK as a function of the average SNR per information bit of the first input branch for different diversity orders

generating polynomial [171,133], and soft decision Viterbi decoding with decoding depth equal to 64. Our LDPC code with higher code rate ($R = 0.75$) performs better than CC(2,1,7). For example, at a BER of 10^{-6} , the LDPC code outperforms convolutional code by about 1.9 dB for all values of parameter α .

The comparison between the LDPC-coded MRC and EGC receiver performance is presented in Fig. 9. The superiority of the MRC related to the EGC is more pronounced in channels with deep fading. At a BER of 10^{-6} , when $\alpha = 4$, the MRC requires only 0.15 dB

Table 1 Required γ_{b1} values (in decibels) in order to achieve specified BER values for different diversity orders

BER	10^{-4}		10^{-5}		10^{-6}	
	Uncoded	Coded	Uncoded	Coded	Uncoded	Coded
L						
1		4.8		4.9		5.0
2	10.5	1.1	14.3	1.3		1.4
3	7.2	-0.7	9.4	-0.6	11.7	-0.4
4	5.4	-1.8	7.3	-1.7	9.0	-1.6
5	4.3	-2.6	6.0	-2.5	7.5	-2.4
6	3.4	-3.2	5.0	-3.1	6.5	-3.0

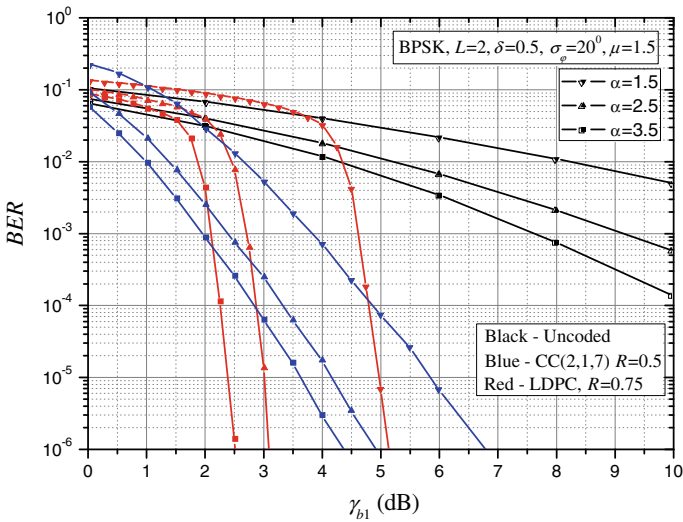


Fig. 8 BER of uncoded and coded BPSK as a function of the average SNR per information bit of the first input branch for different values of fading severity

lower SNR value in comparison with the EGC, while in the case of deep fading, when $\alpha = 1$, the MRC outperforms the EGC even by 1.7 dB.

4 Summary

In this paper, we have studied the performance of uncoded and LDPC-coded EGC receiver operating over generalized fading channel assuming imperfect cophasing and receiver branch imbalance. We have presented the results showing how much the QPSK modulation format is more sensitive to the phase error than the BPSK modulation format in the observed scenario. Also, we have emphasized the range of SNR values when receiver unbalance parameter value has considerable influence on BER performance and showed that receiver unbalance parameter does not influence the BER floor value.

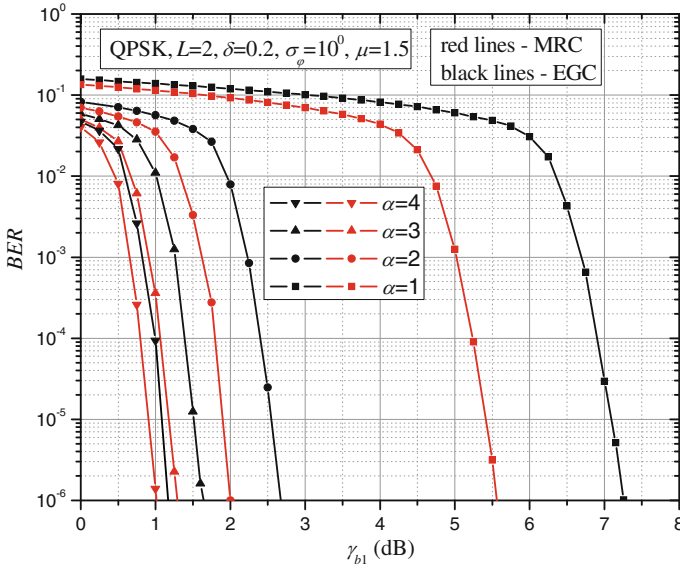


Fig. 9 BER performance of MRC and EGC receiver for different values of fading severity

The regular LDPC code with moderate length and high code rate ($R = 0.75$) suitable for communication over this type system has been designed using the concept of quasi-cyclic LDPC codes of large girth. The results have shown that this LDPC code provides significant coding gain with respect to an uncoded system in generalized fading channel and also is very tolerant to imperfect cophasing. The proposed LDPC code with code rate 0.75 outperforms the convolutional code with code rate 0.5 under previously mentioned influences. We have illustrated that 25 iterations in sum-product LDPC decoding algorithm are sufficient for application of the proposed LDPC code in this system. Furthermore, the influence of LDPC code length on BER performance was investigated and the simulation results have shown that there is no need to increase the codeword length greater than 8074 because little improvements in coding gain are obtained compared to 7166 codeword length. The determined results also enable us to make compromise between the quality of the signal transmission (BER values) and the system complexity (the number of the receiver branches) for uncoded and LDPC coded signaling.

We have observed performance of EGC receiver because it has lower implementation complexity than MRC, and on the other hand as has been shown at BER of 10^{-6} the MRC outperforms EGC of about 0.15 to 1.7 dB depending on fading severity. Moreover, imperfect cophasing in the receiver also suggests lower complexity. The encoding algorithm of suggested LDPC codes can be implemented based on shift-registers and modulo-2 adders, and decoding is based on sum-product that is suitable for FPGA and VLSI implementation.

Acknowledgments The authors thank the anonymous reviewers for their valuable suggestions and comments. This paper was supported in part by the Ministry of Science of Republic of Serbia under technology development project TR-32028—“Advanced techniques for efficient use of spectrum in wireless systems” and in part by the Telenor foundation. It was also supported in part by National Science Foundation (NSF) under grants CCF-0952711, ECCS-0725405 and EEC-0812072.

References

1. Simon, M. K., & Alouini, M. S. (2005). *Digital communication over fading channels* (2nd ed.). New York: Wiley.
2. Beaulieu, N. C., & Abu-Dayya, A. A. (1991). Analysis of equal gain diversity on Nakagami fading channels. *IEEE Transactions on Communications*, 39(2), 225–234.
3. Zogas, D. A., Karagiannidis, G. K., & Kotsopoulos, S. A. (2005). Equal gain combining over Nakagami- n (Rice) and Nakagami- q (Hoyt) generalized fading channels. *IEEE Transactions on Wireless Communications*, 4(2), 374–379.
4. Sagias, N. C., Karagiannidis, G. K., Mathiopoulos, P. T., & Tsiftsis, T. A. (2006). On the performance analysis of equal-gain diversity receivers over generalized Gamma fading channels. *IEEE Transactions on Wireless Communications*, 5(10), 2967–2975.
5. Piboongunon, T., Aalo, V. A., & Iskander, C.-D. (2005). Average error rate of linear diversity reception schemes over generalized Gamma fading channels. *Proceedings of the IEEE SoutheastCon*, 265–270.
6. Najib, M. A., & Prabhu, V. K. (2000). Analysis of equal-gain diversity with partially coherent fading signals. *IEEE Transactions on Vehicular Technology*, 49(3), 783–791.
7. Sagias, N. C., & Karagiannidis, G. K. (2005). Effects of carrier phase error on EGC receivers in correlated Nakagami- m fading. *IEEE Communication Letters*, 9(7), 580–582.
8. Smadi, M. A., & Prabhu, V. K. (2006). Performance analysis of generalized-faded coherent PSK channels with equal-gain combining and carrier phase error. *IEEE Transactions on Wireless Communications*, 5(3), 509–513.
9. Yacoub, M. D. (2002). The $\alpha - \mu$ distribution: A general fading distribution. *Proceedings of IEEE International Symposium on Personal, Indoor and Mobile Radio Communications*, 2, 629–633.
10. Yacoub, M. D. (2007). The $\alpha - \mu$ distribution: A physical fading model for the Stacy distribution. *IEEE Transactions on Vehicular Technology*, 56(1), 27–34.
11. Lindsey, W. C., & Simon, M. K. (1972). *Telecommunication systems engineering*. New Jersey: Prentice-Hall.
12. Gradshteyn, I. S., & Ryzhik, I. M. (2000). *Table of integrals, series, and products* (6th ed.). New York: Academic.
13. Fossorier, M. P. C. (2004). Quasi-cyclic low-density parity-check codes from circulant permutation matrices. *IEEE Transactions on Information Theory*, 50(8), 1788–1793.
14. Djordjevic, I. B., Xu, L., Wang, T., & Cvijetic, M. (2008). Large girth low-density parity-check codes for long-haul high-speed optical communications. In *Proceedings of OFC/NFOEC 2008*, San Diego, CA, Paper no. JWA53.
15. Tanner, R. (1981). A recursive approach to low complexity codes. *IEEE Transactions on Information Theory*, 27(5), 533–547.
16. Xiao-Yu, H., Eleftheriou, E., Arnold, D.-M., & Dholakia, A. (2001). Efficient implementations of the sum-product algorithm for decoding of LDPC codes. *Proceedings of IEEE Globecom 2001*, 2, 1036–1036E.
17. Marsaglia, G., & Tsang, W. W. (2000). A simple method for generating gamma variables. *ACM Transactions on Mathematical Software*, 26(3), 363–372.
18. Kundu, D., & Gupta, R. D. (2007). A convenient way of generating gamma random variables using generalized exponential distribution. *Computational Statistics & Data Analysis*, 51(6), 2796–2802.
19. Jeruchim, M. C., Balaban, P., & Shanmugan, K. S. (2000). *Simulation of communication systems—modeling, methodology, and techniques*. Netherlands: Kluwer.
20. Press, W. H., Teukolsky, S. A., Vetterling, W. T., & Flannery, B. P. (2002). *Numerical recipes in C* (2nd ed.). Cambridge: Cambridge University Press.

Author Biographies



Goran T. Djordjevic was born in Nis, Serbia. He received his B.S., M.S., and Ph.D. degrees in electrical engineering from the Faculty of Electronic Engineering, University of Nis, Serbia, in 1996, 1999 and 2005, respectively. His area of interest is communication theory and applications in satellite, wireless and optical communication systems. His current research interests include application of different modulation formats and error control codes in satellite fixed and mobile services, modeling and simulation of fading channels, synchronization problems. Currently he is an Assistant Professor at the Department of Telecommunications, Faculty of Electronic Engineering, University of Nis, Serbia. He teaches courses of Statistical Communication Theory, Modeling and Simulation of Communication Systems, Information Theory and Satellite Communications. Dr. Djordjevic is a recipient of the 2005 Best Young Scientists Paper Award at the 49th ETRAN Conference and 2007 Prof. Dr. Ilija Stojanovic Award for the contribution in the field of communications.



Ivan B. Djordjevic is an Assistant Professor in the Department of Electrical and Computer Engineering, with a joint appointment in the College of Optical Sciences. Prior to this appointment in August 2006, he was with University of Arizona, Tucson, USA (as a Research Assistant Professor); University of the West of England, Bristol, UK; University of Bristol, Bristol, UK; Tyco Telecommunications, Eatontown, USA; and National Technical University of Athens, Athens, Greece. His current research interests include optical networks, error control coding, constrained coding, coded modulation, turbo equalization, OFDM applications, and quantum error correction. He presently directs the Optical Communications Systems Laboratory (OCSL) within the ECE Department at the University of Arizona. Dr. Djordjevic is an author, together with Dr. William Shieh, of the book *OFDM for Optical Communications*, Elsevier, Oct. 2009. He is also an author, together with Professors Ryan and Vasic, of the book *Coding for Optical Channels*, Springer, Mar. 2010. Dr. Djordjevic is an author of over 120

journal publications and over 120 conference papers. Dr. Djordjevic serves as an Associate Editor for *International Journal of Optics*. Dr. Djordjevic is the IEEE Senior Member and the OSA Member.



George K. Karagiannidis (M'97-SM'04) was born in Pithagorion, Samos Island, Greece. He received the University and Ph.D. degrees in electrical engineering from the University of Patras, Patras, Greece, in 1987 and 1999, respectively. From 2000 to 2004, he was a Senior Researcher at the Institute for Space Applications and Remote Sensing, National Observatory of Athens, Greece. In June 2004, he joined Aristotle University of Thessaloniki, Thessaloniki, Greece, where he is currently Associate Professor on Digital Communication Systems, in the Electrical and Computer Engineering Department. His current research interests include wireless communication theory, digital communications over fading channels, cooperative diversity systems, cognitive radio, satellite communications, and wireless optical communications. He is the author or coauthor of more than 90 technical papers published in scientific journals and presented at international conferences. He is also a coauthor of two chapters in books and a coauthor of the Greek edition of a book on mobile communications. He serves on the editorial board of the *EURASIP JOURNAL ON WIRELESS*

COMMUNICATIONS AND NETWORKING. Dr. Karagiannidis has been a member of Technical Program

Committees for several IEEE conferences. He is a member of the editorial boards of the IEEE TRANSACTIONS ON COMMUNICATIONS and the IEEE COMMUNICATIONS LETTERS. He is co-recipient of the Best Paper Award of the Wireless Communications Symposium (WCS) in IEEE International Conference on Communications (ICC' 07), Glasgow, U.K., June 2007.